BRIEF REPORT

Complete mitochondrial genome assembly of two searobin species (genus *Prionotus*) and their phylogenetic relationships (Triglidae: Prionotinae)

Alan Marín[1], Ruben Alfaro[2], Eliana Zelada-Mázmela[1]

[1] *Laboratorio de Genética, Fisiología y Reproducción, Facultad de Ciencias, Universidad Nacional del Santa, Chimbote, Perú*

[2] *Ecobiotech Lab S.A.C. Trujillo, Perú*

Corresponding author: Alan Marín amarin@uns.edu.pe

Abstract

Background The genus *Prionotus* "searobins" are marine ray-finned fish of the subfamily Prionotinae that have evolved distinctive morphological features and specialized behavior for walking over the seafloor detecting buried preys, making them excellent candidates for biological models in evolutionary genetics studies. Despite that, their phylogenetic relationships are still not well understood. Here, we assembled the first complete mitochondrial genomes of two searobin species namely *Prionotus alatus* and *P. stephanophrys* and performed a comparative mitogenome examination including the first phylogenetic analysis of Prionotinae based on complete mitogenomic information.

Methods and results Both mitogenomes were assembled using Illumina genomic reads mined from the GenBank database. Single circular contigs of 16,602 and 16,896 bp were obtained for *P. alatus* and *P. stephanophrys* respectively. Both mitogenomes displayed a standard vertebrate organization (13 PCGs, 2 rRNAs, 22 tRNAs, and a putative control region) except for a third tRNA-Leu and an extra non-coding region detected in *P. stephanophrys*. A Bayesian phylogenetic analysis recovered all *Prionotus* species into a monophyletic clade within Prionotinae, including the sister taxon *Bellator* grouped in a discrete subclade. Species of the subfamily Triglinae were resolved in a basal monophyletic group within Triglidae.

Conclusion The results presented herein represent an important step into a deeper understanding of the phylogenetic relationships and evolution of *Prionotus*. Taxonomic clarification may also support future management and conservation efforts of these economically valuable species.

Keywords: Mitogenomics, Phylogeny, Scorpaenoidei, GenBank data mining

Introduction

Species of the genus *Prionotus* Lacepède, 1801 (Triglidae: Prionotinae), commonly known as "searobins", not only support important fisheries throughout their distribution ranges but also possess specialized morphological and biological characteristics such as wing-like pectoral fins with three modified lower rays used to "walk" along the sea bottom and certain species use those rays to detect buried preys due to their sensitiveness to chemical and mechanical stimuli (Portnoy et al., 2017; Allard et al., 2024). Such unique features make them ideal biological models for evolutionary genetics and adaptation studies (Herbert et al., 2024).

According to the World Register of Marine Species (WORMS) database, there are currently 23 extant *Prionotus* species (Froese and Pauly, 2025), whose natural distribution is restricted to the Americas (Portnoy et al., 2017), including 16 western Atlantic and 7 eastern Pacific species. Nevertheless, taxonomic research on the classification of *Prionotus* remains scarce, and only a few studies have addressed their taxonomy using morphological characters (Imamura, 1996; Richards and Jones, 2002), while only two studies performed molecular phylogenetic analysis employing information from partial mitochondrial and nuclear gene fragments (Portnoy et al., 2017; Smith et al., 2018). Although there has been some degree of consistency between the results of prior morphological and molecular phylogeny studies, the molecular phylogenetic results of Portnoy et al. (2017) rendered *Prionotus* as paraphyletic within Triglidae, suggesting that the currently accepted genus *Bellator*, its only sister genus within the subfamily Prionotinae, should be considered as a junior synonym of *Prionotus* until further studies using robust phylogenetic analysis and broader species coverage shed much additional light on the taxonomic status of Prionotinae species.

Since phylogeny relationships inferred from morphological characters and/or partial gene fragments may lead to limited taxonomic resolution, the use of more robust genome-wide data has become necessary to resolve complex phylogenetic problems in fish lineages (Miya and

Nishida, 2015). In this context, nucleotide information obtained from the complete mitogenome has proven effective in resolving the phylogeny of several fish taxa on many taxonomic levels (Miya and Nishida, 2015). Moreover, the unique properties of the mitogenome (e.g. fast evolutionary rates, lack of recombination, high copy number) make this organelle a great source of powerful molecular markers suitable for diverse applications including accurate species identification, wildlife forensics, environmental DNA, population genetics and evolutionary studies (Maduna et al., 2022).

Despite the existence of 6 mitogenomes from Atlantic *Prionotus* species available in the GenBank database and the unresolved taxonomic status of Prionotinae species, no study has yet analyzed those mitogenomes to investigate their phylogenetic relationships. Furthermore, the vast amount of genomic next-generation sequencing (NGS) data publicly available within the GenBank database provides a rich source of organelle genomes that can be screened to identify fish species of taxonomic interest (Eldem et al., 2024; Marín et al., 2025). The objective of the present work was: a) to assemble the mitochondrial genomes of two commercially important searobin species namely *P. alatus* and *P. stephanophrys* using SRA reads mined from GenBank, b) to describe the mitogenome characteristics and perform comparative analyses, and c) to investigate the phylogenetic relationships of Triglidae species using the two *Prionotus* mitogenomes assembled herein and the mitogenomes of all Triglidae species available in GenBank.

Materials and methods

Genomic NGS reads mining, mitogenome assembly and annotation

The NGS reads used to assemble the two mitochondrial genomes came from two BioSamples deposited in the GenBank database. BioSample metadata records indicate that the *P. alatus*

107 (BioSample SAMN36762230) and the *P. stephanophrys* (BioSample SAMN31811746)
108 individuals were collected from the Atlantic Ocean in USA (34.6094 N, 75.7052 W) on
109 September 17, 2022, and from the Pacific Ocean in El Salvador (12.7459 N, 89.0088 W) on
110 December 10, 2010, respectively, by the Smithsonian National Museum of Natural History in
111 their "NOAA Genome Skimming of Marine animals inhabiting the US Exclusive Economic
112 Zone" project (BioProject accession PRJNA720393). Paired-end FASTQ genomic reads
113 (Platform: Illumina NovaSeq 6000, *P. alatus*: 1.9 Gbp within 12.50 million reads; *P.*
114 *stephanophrys*: 1.8 Gbp within 12.13 million reads) were downloaded from the public
115 GenBank SRA repository (*P. alatus* SRA accession SRR25465369; *P. stephanophrys* SRA
116 accession SRR22396965). Raw reads were subjected to quality control using FastQC and
117 trimmed with BBDuk as implemented in Geneious Prime v. 2025.0 (Biomatters Ltd., Auckland,
118 New Zealand) resulting in 12.49 and 12.07 million reads in *P. alatus* and *P. stephanophrys*
119 respectively. To validate the mitogenomes assembled herein, we obtained consensus
120 mitogenomes from two different strategies namely "map to reference" approach and a hybrid
121 "map to reference/de novo" approach. For the first approach, trimmed reads from *P. alatus* and
122 *P. stephanophrys* were assembled against the complete mitogenome reference sequences of *P.*
123 *nudigula* (GenBank accession NC_088019) and *P. evolans* (GenBank accession NC_083024)
124 respectively, using the "Map to Reference" tool in Geneious Prime with default parameter
125 settings recommended by the software developers (Sensitivity: Medium-Low Sensitivity/Fast,
126 five iterations). For the second approach, the contigs obtained from the first assembly approach
127 were dissolved and reassembled "de novo" following the parameter settings recommended by
128 the software developers (Sensitivity: Medium Sensitivity/Fast) and selecting the "circularize
129 contigs" option. The consensus sequences obtained from both approaches were extracted and
130 checked manually using the Genious Prime alignment tool.

131 Gene annotation was performed using the "Annotate and Predict" feature of Geneious Prime
132 by comparing the novel *P. alatus* and *P. stephanophrys* mitogenomes to other complete
133 mitogenomes of closely related species. The start and stop codon positions of the protein-
134 coding genes (PCGs) were verified using the Open Reading Frame Finder tool (available at
135 https://www.ncbi.nlm.nih.gov/orffinder/) using the vertebrate mitochondrial genetic code. The
136 positions of the transfer RNA genes (tRNAs) were verified using tRNAscan-SE (Chan and
137 Lowe 2019). The circular mitogenome figures were generated with Organellar Genome Draw
138 "OGDRAW" version 1.3.1 (Greiner et al., 2019) and edited with Inkscape macOS version 1.4
139 (Inkscape Project, 2020).
140

141 **Bayesian phylogenetic analysis**

142 For the Bayesian phylogenetic analysis, we used the 13 PCGs of the two mitogenomes
143 assembled herein plus those of all Triglidae species available in GenBank (17 species: 8 from
144 Prionotinae and 9 from Triglinae). A Hoplichthyidae species, *Hoplichthys gilberti*, was used
145 as outgroup. Nucleotide sequences from each PCG were multialigned separately using MEGA
146 7 (Kumar et al., 2016) and concatenated with SeaView version 5.0.4 (Guoy et al., 2021),
147 resulting in a final matrix of 11,444 nucleotides. The program jModelTest 2 (Darriba et al.,
148 2012) was used to find the most appropriate model of nucleotide evolution for each one of the
149 13 PCGs under the corrected Bayesian Information Criterion (BICc). Levels of substitution
150 saturation at single codon positions from each PCG were assessed with Xia´s method
151 implemented in DAMBE7 (Xia, 2018). The third codon positions of three PCGs (ATP8,
152 NADH3, and NADH6) showed clear signs of saturations and thereby the Bayesian analysis
153 was run with the data partitioned by gene and by codon position excluding the third codon
154 position of those genes. Bayesian phylogenetic trees were constructed with MrBayes 3.2.7
155 (Ronquist et al., 2012) as implemented on the CIPRES science gateway 3.3 server (Miller et

156 al. 2010), using two independent runs of four Markov chains each, conducted for 10,000,000
157 generations, with samplings frequency of 1000. The first 25% of the sampled trees were
158 discarded as burn-in. The final consensus phylogenetic tree was drawn using Figtree version
159 1.4.4 (http://tree.bio.ed.ac.uk/software/figtree/).
160
161

162 **Results and discussion**

163 In this study, we successfully assembled and annotated the first mitochondrial genomes of the
164 Atlantic spiny searobin *P. alatus* (occurring from the western Atlantic from Virginia in the
165 USA to the Campeche Shelf in Mexico) and the Pacific lumptail searobin *P. stephanophrys*
166 (occurring from the Columbia River in Washington in the USA to Ilo in Peru) (Russell et al.,
167 1992; Chirichigno and Cornejo, 2001). There were no differences between the consensus
168 mitogenome contigs obtained with the two different assembly approaches applied herein. A
169 total of 30,235 trimmed reads from *P. alatus* and 24,089 from *P. stephanophrys* were
170 assembled against the selected reference sequences, allowing the generation of a single circular
171 contig of 16,602 bp in length (mean per base coverage of 121.2 reads) in *P. alatus* and 16,896
172 bp (mean per base coverage of 133.1 reads) in *P. stephanophrys* (GenBank accessions pending)
173 (Fig. 1), which were within the size range of other reported *Prionotus* mitogenomes ranging
174 from 16,599 bp in *P. nudigula* (NC_088019.1) to 16,907 in *P. evolans* (NC_083024.1). Overall,
175 the novel mitogenome sequences showed highly similar base frequencies of A=26.3%,
176 C=29.6%, G=17.3%, and T=26.8% in *P. alatus* and of A=26.6%, C= 29.6%, G=17.6%, and
177 T=26.2% in *P. stephanophrys*.
178

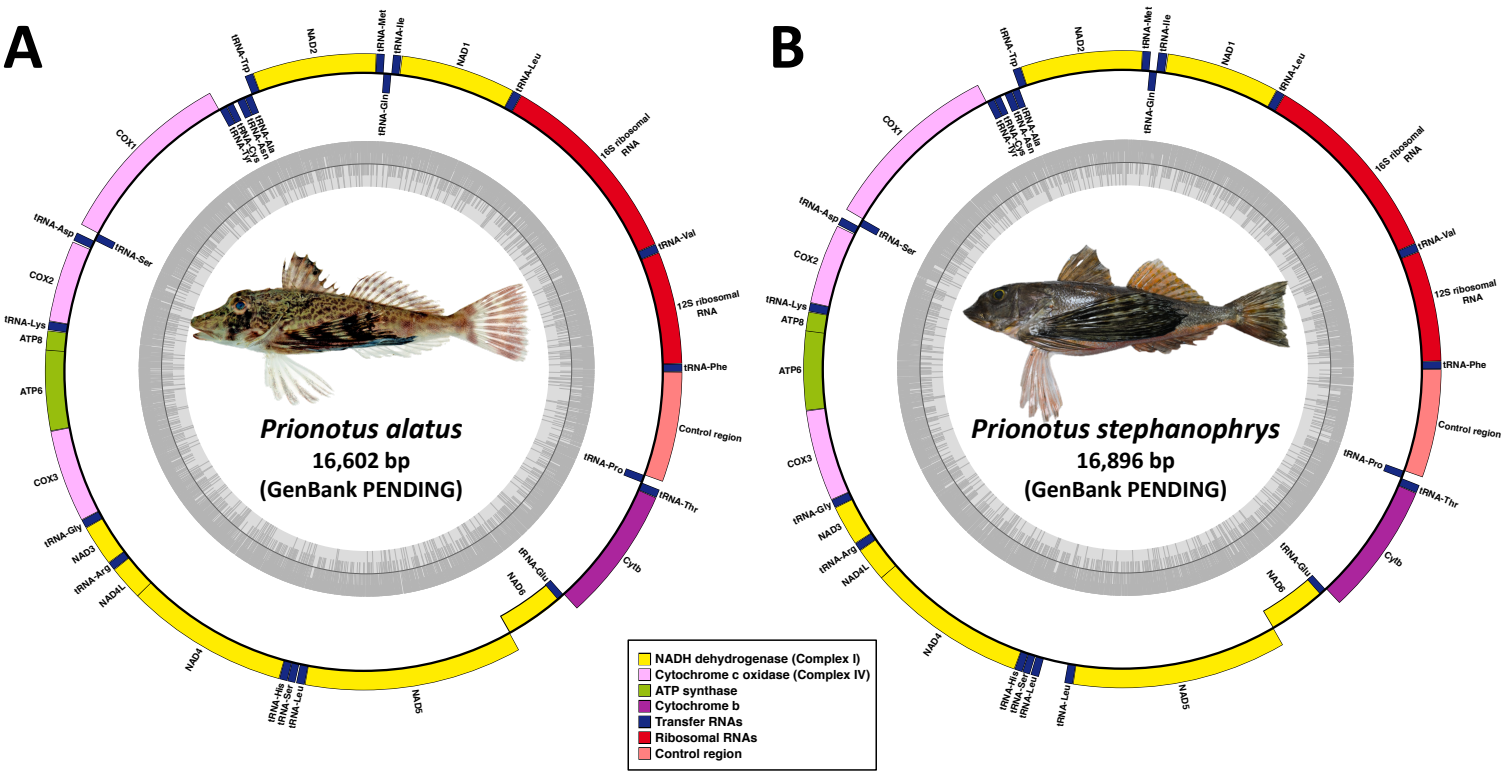

Fig. 1. Circular mitochondrial genome organization of A) *P. alatus* (photo kindly provided by R. Robertson, Robertson and Van Tassell, 2015) and B) *P. stephanophrys* (Photo by R. Alfaro). Genes inside the circle (negative strand) are transcribed clockwise and genes outside the circle counter clockwise. The circle inside the GC content graph (innermost circle) indicates the 50% threshold where darker and lighter grey corresponds to the GC and AT content respectively. NADH dehydrogenase, cytochrome c oxidase, ATP synthase, transfer RNA, and ribosomal RNA genes are depicted in yellow, pink, green, purple, blue, and red bars respectively. The bar representing the control region is shown in coral red color.

Both mitogenomes showed a standard vertebrate organization (i.e. 13 PCGs, 2 rRNAs, 22 tRNAs, and a putative control region) (Winn et al., 2024), except for a third tRNA-Leu and an extra non-coding region detected in the mitogenome of *P. stephanophrys*. The third tRNA-Leu was located in the positive strand between a 220 bp non-coding region downstream of the conserved block NADH4/His/Ser/Leu and the NADH5 gene (Table 1 and Fig. 1). This unusual

193 **Table 1.** Complete mitochondrial annotation and number of amino acids in each of the genes
194 detected in the mitochondrial genomes of *Prionotus alatus* (PA) and *P. stephanophrys* (PS).
195 The plus "+" and minus "-" signs stand for the heavy and light strands respectively. NCR: non-
196 coding region.

Gene	Strand	Location				Size (bp)		Anticodon		START codon		STOP codon		No. of amino acids	
		Start		End											
		PA	PS	PA	PS	PA	PS	PA	PS	PA	PS	PA	PS	PA	PS
Phe (F)	+	1	1	68	68	68	68	GAA	GAA	—	—	—	—	—	—
12S rRNA	+	69	69	1016	1017	948	949	—	—	—	—	—	—	—	—
Val (V)	+	1017	1018	1090	1091	74	74	UAC	UAC	—	—	—	—	—	—
16S rRNA	+	1091	1092	2782	2789	1692	1698	—	—	—	—	—	—	—	—
Leu (L)	+	2783	2790	2856	2863	74	74	UAA	UAA	—	—	—	—	—	—
NADH1	+	2857	2864	3831	3833	975	975	—	—	ATG	ATG	TAA	TAG	324	324
Ile (I)	+	3836	3843	3905	3912	70	70	GAU	GAU	—	—	—	—	—	—
Gln (Q)	-	3905	3912	3975	3982	71	71	UUG	UUG	—	—	—	—	—	—
Met (M)	+	3975	3982	4043	4051	69	70	CAU	CAU	—	—	—	—	—	—
NADH2	+	4044	4052	5089	5097	1046	1046	—	—	ATG	ATG	TA-	TA-	348	348
Trp (W)	+	5090	5098	5161	5168	72	71	UCA	UCA	—	—	—	—	—	—
Ala (A)	-	5163	5170	5231	5238	69	69	UGC	UGC	—	—	—	—	—	—
Asn (N)	-	5233	5440	5305	5312	73	73	GUU	GUU	—	—	—	—	—	—
Cys (C)	-	5344	5351	5408	5415	65	65	GCA	GCA	—	—	—	—	—	—
Tyr (Y)	-	5409	5416	5478	5485	70	70	GUA	GUA	—	—	—	—	—	—
COI	+	5480	5487	7030	7037	1551	1551	—	—	GTG	GTG	TAA	TAA	516	516
Ser (S)	-	7031	7038	7101	7108	71	71	UGA	UGA	—	—	—	—	—	—
Asp (D)	+	7105	7112	7177	7184	73	73	GUC	GUC	—	—	—	—	—	—
COII	+	7188	7193	7878	7883	691	691	—	—	ATG	ATG	T--	T--	230	230
Lys (K)	+	7879	7884	7952	7957	74	74	UUU	UUU	—	—	—	—	—	—
ATP8	+	7956	7959	8123	8126	168	168	—	—	ATG	ATG	TAA	TAA	55	55
ATP6	+	8114	8117	8796	8799	683	683	—	—	ATG	ATG	TA-	TA-	227	227
COIII	+	8797	800	9581	9584	785	785	—	—	ATG	ATG	TA-	TA-	261	261
Gly (G)	+	9582	9585	9653	9655	72	71	UCC	UCC	—	—	—	—	—	—
NADH3	+	9654	9656	10002	10004	349	349	—	—	ATG	ATG	T--	T--	116	116
Arg (R)	+	10003	10005	10071	10073	69	69	UCG	UCG	—	—	—	—	—	—
NADH4L	+	10072	10074	10368	10370	297	297	—	—	ATG	ATG	TAA	TAA	98	98
NADH4	+	10362	10364	11742	11744	1381	1381	—	—	ATG	ATG	T--	T--	460	460
His (H)	+	11743	11745	11812	11813	70	69	GUG	GUG	—	—	—	—	—	—
Ser (S)	+	11813	11814	11879	11880	67	67	GCU	GCU	—	—	—	—	—	—
Leu (L)	+	11887	11887	11959	11959	73	73	UAG	UAG	—	—	—	—	—	—
NCR	+/-	—	11960	—	12179	—	220	—	—	—	—	—	—	—	—
Leu (L)	+	—	12180	—	12252	—	73	—	UAG	—	—	—	—	—	—
NADH5	+	11960	12253	13798	14091	1839	1839	—	—	ATG	ATG	AGA	TAA	612	612
NADH6	-	13794	14088	14315	14609	522	522	—	—	ATG	ATG	TAG	TAA	173	173
Glu (E)	-	14316	14610	14384	14677	69	68	UUC	UUC	—	—	—	—	—	—
CYTb	+	14388	14683	15528	15823	1141	1141	—	—	ATG	ATG	T--	T--	380	380
Thr (T)	+	15529	15824	15600	15895	72	72	UGU	UGU	—	—	—	—	—	—
Pro (P)	-	15601	15896	15670	15965	70	70	UGG	UGG	—	—	—	—	—	—
Control region	+	15671	15696	16602	16896	932	1200	—	—	—	—	—	—	—	—

197

198

199

200 non-coding region was also observed in the mitogenomes of *P. rubio* (219 bp), *P. tribulus* (219
201 bp), and *P. evolans* (235 bp). Similarly, a non-coding region of 533 bp and 165 bp were
202 reported within the cluster NADH4/His/Ser/Leu/NADH5 in the freshwater gobioid
203 *Odontobutis platycephala* (GenBank accession NC_010199; Ki et al., 2008) and in the
204 threadfin *Eleutheronema rhadinum* (Genbank accession MW845829; Zhong et al., 2021)
205 respectively. Although the unusual non-coding region observed in the four previously
206 mentioned *Prionotus* species may have been formed as a result of an unknown evolutionary
207 process due to their close phylogenetic relationship (Fig. 2), we cannot rule out the possibility
208 of an artefactual origin due to the presence of a C homopolymer at the 5' end of this non-coding
209 region, which is known to bias short read sequencing (Laehnemann et al., 2016).
210 The size of the PCGs ranged from 168 bp (55 amino acids) in the ATP8 to 1,839 (612 amino
211 acids) in the NADH5 of both mitogenomes. All PCGs were encoded in the heavy strand, except
212 for the NADH6 which was encoded in the light strand. Most PCGs of both mitogenomes used
213 the start codon ATG, except for the COI gene which was initiated with the alternative GTG
214 codon. The use of alternative stop codons was observed only in two genes of *P. alatus*
215 mitogenome where the NADH5 and NADH6 genes ended with the AGA and TAG codons
216 respectively, and the NADH1 gene in *P. stephanophrys* that used the stop codon TAG. In both
217 mitogenomes, the heavy strand contained the two rRNA and 14 tRNA genes, including the
218 additional tRNA-Leu detected in *P. stephanophrys*, while the light strand contained the
219 remaining 8 tRNA genes.
220 The Bayesian phylogenetic analysis recovered high to maximum statistical support in all clades
221 (Fig. 2), grouping all *Prionotus* and *Bellator* species within a major Prionotinae clade. The 8
222 analyzed *Prionotus* species were recovered within three discrete subclades indicated from
223 apical towards more basal positions within the phylogenetic tree: subclade I) *P. rubio* + *P.*
224 *tribulus* + *P. evolans* + *P. stephanophrys*, subclade II) *P. carolinus* + *P. scitulus*, and subclade

III) *P. alatus* + *P. nudigula*. The *Bellator* subclade (*B. egretta* + *B. brachychir*) was positioned at the basal node of Prionotinae. The well supported sister relationship between *Prionotus* and *Bellator* supports the current accepted genus status of *Bellator*, which is also in agreement with the results of the morphological taxonomic analysis reported by Miller and Richards (1991) and Imamura (1996). In our phylogenetic results, the subfamily Triglinae, which consisted of 9 species within 3 genera (*Chelidonichthys*, *Eutrigla*, and *Lepidotrigla*), was recovered in the basal position of the phylogenetic tree. These results support the molecular phylogeny of Portnoy et al. (2017), where the Triglinae group was regarded as more basal than Prionotinae. However, our results are in disagreement with those of Richards an Jones (2002), whose morphological phylogeny analysis recovered *Prionotus* and *Bellator* in adjacent but different clades, identifying the Prionotinae as the most ancestral subfamily within Triglidae. In contrast to our findings, the results of Portnoy et al. (2017) rendered *Prionotus* as paraphyletic within Prionotinae with *Bellator* recovered within the genus *Prionotus*. To address this issue, the authors suggested two alternative solutions: to retain *Bellator* and split *Prionotus* into different genera or to lump *Bellator* into the *Prionotus* genus.

Our results recovered *P. alatus* and *P. stephanophrys* within different subclades of Prionotinae, showing the closest relationships with *P. nudigula* and *P. evolans* respectively. The estimated levels of divergence (Kimura two-parameter model) between *P. alatus*-*P. nudigula* and *P. stephanophrys*-*P. evolans* were 0.05 and 0.12 respectively. Taking into account that *P. stephanophrys* was the only Pacific species included in our study and that there are still several Atlantic species without sequenced mitogenomes, our results cannot determine which Atlantic species represent the transisthmian sister taxon of *P. stephanophrys*. However, based on the results reported by Portnoy et al. (2017), *P. longispinosus* represents so far, the closest Atlantic relative of *P. stephanophrys*, and likely the transisthmian sister species of *P. stephanophrys*.

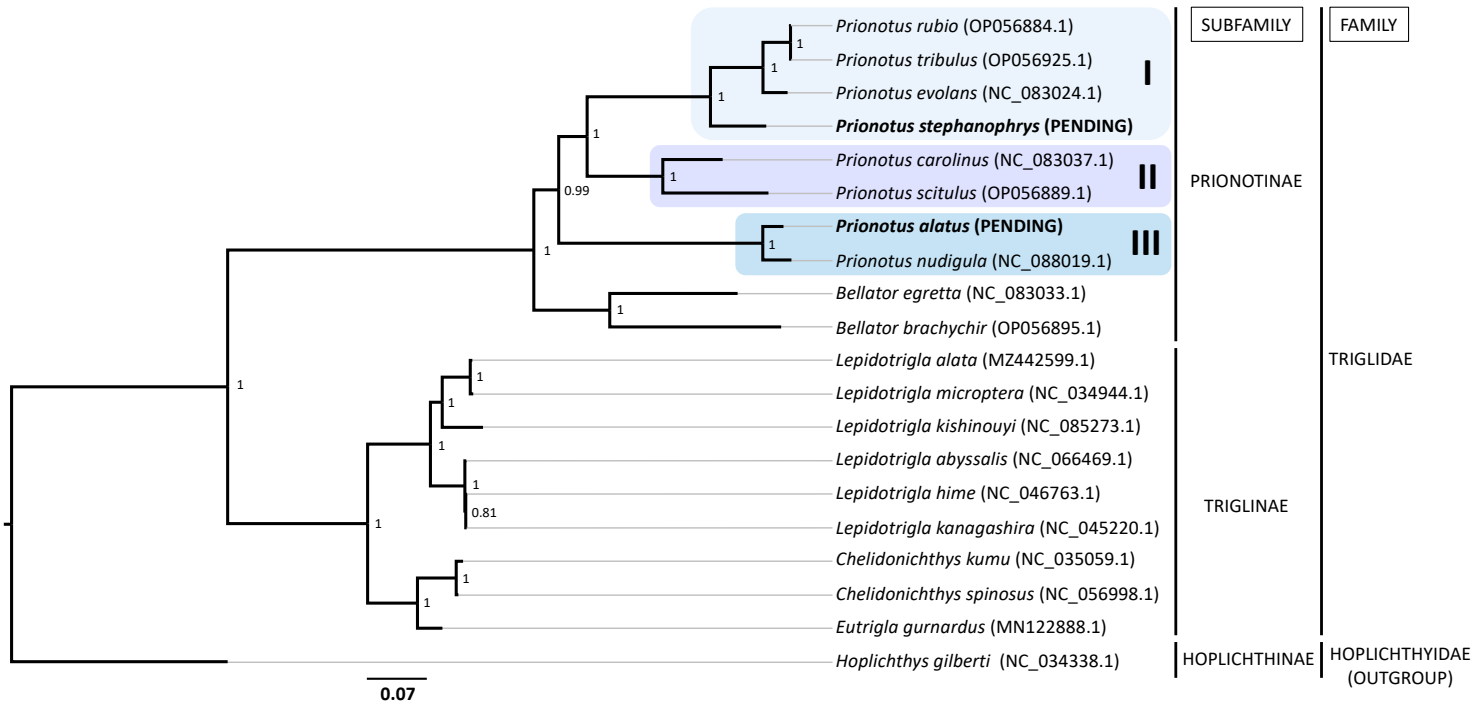

Fig. 2. Bayesian phylogenetic tree constructed based on the concatenation of 13 mitochondrial protein-coding genes of 19 Triglidae species (GenBank accessions are shown between parenthesis). The two species with newly determined mitogenomes assembled in this study (*Prionotus alatus* and *P. stephanophrys*, subfamily Prionotinae) are highlighted in bold. The three subclades formed by *Prionotus* species are shaded in sky blue, violet, and blue respectively. Posterior probabilities are shown at correspondent nodes. The Gilbert's spiny flathead *Hoplichthys gilberti* was used as outgroup.

The shortest interspecific genetic distance (K2P=0.0014; 23 variable sites) was observed between the mitogenomes of *P. rubio* (Genbank accession OP056884, Biosample SAMN29555344) and *P. tribulus* (Genbank accession OP056925, BioSample SAMN29555068), displaying the same length of 16,891 bp. Further analysis of the COI gene sequence of both mitogenomes in the BOLD database identified both sequences as *P. tribulus*. Taken all these results together, it is likely that Biosample SAMN29555344, identified as *P.*

rubio, may be a hybrid between a male *P. rubio* and a female *P. tribulus*. Hybridization between different *Prionotus* species has been previously reported in the wild and under laboratory conditions (McClure and McEachran, 1992; Herbert et al., 2024), which suggests that the possible hybridization between the sympatric *P. rubio* and *P. tribulus* is likely.

Conclusion

The phylogenetic analysis performed herein recovered *Prionotus* and *Bellator* species as sister taxon within Prionotinae, which is in agreement with some previous related studies. The monophyletic condition of *Prionotus* is in disagreement with the findings reported by Portnoy et al. (2017), where *Prionotus* was rendered as paraphyletic, suggesting that *Bellator* should be considered as a junior synonym of *Prionotus*. However, the only two *Bellator* species with complete mitogenomes included in our analysis (*B. egretta* and *B. brachychir*) were different from those analyzed by Portnoy et al. (2017). Thereby, the putative paraphyletic status of *Prionotus* is still uncertain, highlighting the need for the complete mitogenome sequencing of more *Prionotus* and *Bellator* species that may allow robust molecular phylogenetic analysis with broader taxon coverage.

References

Allard CA, Herbert AL, Krueger SP, Liang Q, Walsh BL, Rhyne AL, ... Bellono NW (2024) Evolution of novel sensory organs in fish with legs. Curr Biol 34(19): 4349-4356.

Chirichigno N, Cornejo RM (2001) Catálogo comentado de los peces marinos del Perú. Lima: Instituto del Mar del Perú. 2001: 314 pp.

David S, Stuart C, Dominic G, John R, Kevin W (2017) Molecular phylogenetics of New World searobins (Triglidae; Prionotinae). Mol Phylogenet Evol 107:382-387.

Eldem V, Balcı MA (2024) Mining NCBI Sequence Read Archive Database: An Untapped Source of Organelle Genomes for Taxonomic and Comparative Genomics Research. Divers 16(2): 104.

Froese R, Pauly D Editors (2025) FishBase. Prionotus Lacepède, 1801. Accessed through: World Register of Marine Species at: https://www.marinespecies.org/aphia.php?p=taxdetails&id=159569 on 2025-01-30

Gouy M, Tannier E, Comte N, Parsons DP (2021) Seaview version 5: a multiplatform software for multiple sequence alignment, molecular phylogenetic analyses, and tree reconciliation. Multiple sequence alignment: Methods Protoc 241-260.

Greiner S, Lehwark P, Bock R (2019) OrganellarGenomeDRAW (OGDRAW) version 1.3. 1: expanded toolkit for the graphical visualization of organellar genomes. Nucleic Acids Res 47(W1): W59-W64.

Herbert AL, Allard CA, McCoy MJ, Wucherpfennig JI, Krueger SP, Chen HI, ...Kingsley DM (2024) Ancient developmental genes underlie evolutionary novelties in walking fish. Curr Biol 34(19): 4339-4348.

Imamura H (1996) Phylogeny of the family Platycephalidae and related taxa (Pisces: Scorpaeniformes). Species Divers 1(2): 123-233.

Inkscape Project (2020) Inkscape. Retrieved from https://inkscape.org. Accessed 30 January 2025

Ki JS, Jung SO, Hwang DS, Lee YM, Lee JS (2008) Unusual mitochondrial genome structure of the freshwater goby *Odontobutis platycephala*: rearrangement of tRNAs and an additional non-coding region. J Fish Biol 73(2): 414-428.

311 Kumar S, Stecher G, Tamura K (2016) MEGA7: molecular evolutionary genetics analysis
312 version 7.0 for bigger datasets. Mol Biol Evol 33(7): 1870-1874.

313 Laehnemann D, Borkhardt A, McHardy AC (2016) Denoising DNA deep sequencing data—
314 high-throughput sequencing errors and their correction. Brief Bioinform 17(1): 154-179.

315 Maduna SN, Vivian-Smith A, Jónsdóttir ÓDB, Imsland AK, Klütsch CF, Nyman T, ...Hagen
316 SB (2022) Mitogenomics of the suborder Cottoidei (Teleostei: Perciformes): improved
317 assemblies, mitogenome features, phylogeny, and ecological
318 implications. Genomics 114(2): 110297.

319 Marín A (2025) The first complete mitochondrial genome of the endangered spotted eagle ray
320 *Aetobatus ocellatus*. bioRxiv 2025.01.13.632509.

321 McClure MR, McEachran JD (1992) Hybridization between *Prionotus alatus* and *P. paralatus*
322 in the Northern Gulf of Mexico (Pisces: Triglidae). Copeia 1992(4): 1039-1046.

323 Miya M, Nishida M (2015) The mitogenomic contributions to molecular phylogenetics and
324 evolution of fishes: a 15-year retrospect. Ichthyol Res 62: 29-71.

325 Richards WJ, Jones DL (2002) Preliminary classification of the gurnards (Triglidae:
326 Scorpaeniformes). Mar Freshw Res 53(2): 274-282.

327 Robertson DR, Van Tassell J (2015) Shorefishes of the Greater Caribbean: online information
328 system. Version 3.0 Smithsonian Tropical Research Institute, Balboa, Panamá.

329 Ronquist F, Teslenko M, Van Der Mark P, Ayres DL, Darling A, Höhna S, ...Huelsenbeck JP
330 (2012) MrBayes 3.2: efficient Bayesian phylogenetic inference and model choice across a
331 large model space. Syst Biol 61(3): 539-542.

332 Russell M, Grace M, Gutherz EJ (1992) Field Guide to the searobins (*Prionotus* and *Bellator*)
333 in the western North Atlantic. NOAA Technical Report NMFS 107. U.S. Department of
334 Commerce. March 1992.

335 Smith WL, Everman E, Richardson C (2018) Phylogeny and taxonomy of flatheads,
336 scorpionfishes, sea robins, and stonefishes (Percomorpha: Scorpaeniformes) and the
337 evolution of the lachrymal saber. Copeia 106(1): 94-119.

338 Winn JC, Maduna SN, Bester-van der Merwe AE (2024) A comprehensive phylogenomic
339 study unveils evolutionary patterns and challenges in the mitochondrial genomes of
340 Carcharhiniformes: A focus on Triakidae. Genomics 116(1): 110771.

341 Xia X (2018) DAMBE7: New and improved tools for data analysis in molecular biology and
342 evolution. Mol Biol Evol 35(6): 1550-1552.

343 Zhong L, Wang M, Li D, Tang S, Chen X (2021) Mitochondrial genome of *Eleutheronema*
344 *rhadinum* with an additional non-coding region and novel insights into the
345 phylogenetics. Front Mar Sci 8: 746598.

346

347

348

349

350

351